

Nanoarchitectures Constructed from Resulting Polypseudorotaxanes of the β -Cyclodextrin/4,4'-Dipyridine Inclusion Complex with Co^{2+} and Zn^{2+} Coordination Centers

Yan-Li Zhao,[†] Heng-Yi Zhang, Dong-Sheng Guo, and Yu Liu*

Department of Chemistry, State Key Laboratory of Elemento-Organic Chemistry, Nankai University, Tianjin 300071, P. R. China

Received April 22, 2006. Revised Manuscript Received June 5, 2006

Six supramolecular polypseudorotaxanes (2–7) like the missing link have been constructed by coordination of the β -cyclodextrin/4,4'-dipyridine inclusion complex (1) with cobalt chloride, cobalt acetate, cobalt nitrate, zinc chloride, zinc acetate, and zinc nitrate, respectively, and investigated using ¹H NMR spectroscopy, circular dichroism, FT-IR, gel permeation chromatography, powder X-ray diffraction, thermogravimetric and differential thermal analysis, transmission electron microscopy, and cyclic voltammetry. The obtained results indicate that polypseudorotaxanes 2–7 could self-assemble to form square or rodlike nanostructures. The counteranions play critical roles in the formation of the polypseudorotaxane nanoarchitectures. Especially polypseudorotaxane 2 shows better electrochemical property as compared with that of other polypseudorotaxanes 3–7, which may potentially be used as an electroactive soft material.

Introduction

Using supramolecular technology to control the intermolecular interactions on the molecular level is attracting much attention because of supramolecules' fundamental significance and potential application in the design of functional materials such as soft materials and electronic materials.^{1–4} Electronic materials are often highly reactive, and technological applications are usually limited by a lack of stability. This shortcoming can be improved by the use of a molecular insulating layer. The insulating layer possesses the potential to eliminate the π -interactions and thereby dramatically increase the stability of electronic materials.⁵ Cyclodextrins (CDs) are of special interest because they can be used as cyclic components in the construction of molecular machines

with various molecular catenanes and rotaxanes/polypseudorotaxanes.^{6–22} Especially CDs can also be used as a molecular insulating layer in the construction of the electroactive materials.^{18b,22a} On the other hand, the organic molecular

* To whom correspondence should be addressed. Tel: 86 22-2350-3625. Fax: 86 22-2350-3625. E-mail: yuliu@nankai.edu.cn.

[†] Current address: Department of Chemistry and Biochemistry, University of California, Los Angeles, 607 Charles E. Young Drive East, Los Angeles, CA 90095-1569.

- (1) (a) Ajayan, P. M.; Schadler, L. S.; Braun, P. V. *Nanocomposite Science Technology*; Wiley-VCH Verlag GmbH & Co. KGaA: Weinheim, Germany, 2003. (b) Klabunde, K. J. *Nanoscale Materials in Chemistry*; Wiley-VCH Verlag GmbH & Co. KGaA: Weinheim, Germany, 2001.
- (2) Liang, W.; Shores, M. P.; Bockrath, M.; Long, J. R.; Park, H. *Nature* **2002**, *417*, 725–729.
- (3) (a) Orr, G. W.; Barbour, L. J.; Atwood, J. L. *Science* **1999**, *285*, 1049–1052. (b) Quake, S. R.; Scherer, A. *Science* **2000**, *290*, 1536–1540. (c) Ikkala, O.; ten Brinke, G. *Science* **2002**, *295*, 2407–2409. (d) Jain, S.; Bates, F. S. *Science* **2003**, *300*, 460–464.
- (4) (a) Bong, D. T.; Clark, T. D.; Granja, J. R.; Ghadiri, M. R. *Angew. Chem., Int. Ed.* **2001**, *40*, 988–1011. (b) van Bommel, K. J. C.; Friggeri, A.; Shinkai, S. *Angew. Chem., Int. Ed.* **2003**, *42*, 980–999. (c) Hamley, I. W. *Angew. Chem., Int. Ed.* **2003**, *42*, 1692–1712. (d) Hamley, I. W. *Soft Matter* **2005**, *1*, 36–43. (e) Nayak, S.; Lyon, L. A. *Angew. Chem., Int. Ed.* **2005**, *44*, 7686–7708. (f) Kato, T.; Mizoshita, N.; Kishimoto, K. *Angew. Chem., Int. Ed.* **2006**, *45*, 38–68. (g) Osada, Y.; Gong, J.-P. *Adv. Mater.* **1998**, *10*, 827–837. (h) Liu, J.; Alvarez, J.; Kaifer, A. E. *Adv. Mater.* **2000**, *12*, 1381–1383.
- (5) Swager, T. *Nat. Mater.* **2002**, *1*, 151–152.
- (6) (a) Harada, A. *Acc. Chem. Res.* **2001**, *34*, 456–464. (b) Kawaguchi, Y.; Nishiyama, T.; Okada, M.; Kamachi, M.; Harada, A. *Macromolecules* **2000**, *33*, 4472–4477. (c) Okumura, H.; Kawaguchi, Y.; Harada, A. *Macromolecules* **2003**, *36*, 6422–6429. (d) Takashima, Y.; Oizumi, Y.; Sakamoto, K.; Miyauchi, M.; Kamitori, S.; Harada, A. *Macromolecules* **2004**, *37*, 3962–3964.
- (7) (a) Wang, Q.-C.; Qu, D.-H.; Ren, J.; Chen, K.; Tian, H. *Angew. Chem., Int. Ed.* **2004**, *43*, 2661–2665. (b) Qu, D.-H.; Wang, Q.-C.; Tian, H. *Angew. Chem., Int. Ed.* **2005**, *44*, 5296–5299. (c) Qu, D.-H.; Wang, Q.-C.; Ma, X.; Tian, H. *Chem.-Eur. J.* **2005**, *11*, 5929–5937. (d) Qu, D.-H.; Wang, Q.-C.; Ren, J.; Tian, H. *Org. Lett.* **2004**, *6*, 2085–2088.
- (8) Gu, L.-Q.; Cheley, S.; Bayley, H. *Science* **2001**, *291*, 636–640.
- (9) (a) Nepogodiev, S. A.; Stoddart, J. F. *Chem. Rev.* **1998**, *98*, 1959–1976. (b) Raymo, F. M.; Stoddart, J. F. *Chem. Rev.* **1999**, *99*, 1643–1663. (c) Nelson, A.; Belitsky, J. M.; Vidal, S.; Joiner, C. S.; Baum, L. G.; Stoddart, J. F. *J. Am. Chem. Soc.* **2004**, *126*, 11914–11922. (d) Nelson, A.; Stoddart, J. F. *Org. Lett.* **2003**, *5*, 3783–3786.
- (10) Murakami, H.; Kawabuchi, A.; Kotoo, K.; Kunitake, M.; Nakashima, N. *J. Am. Chem. Soc.* **1997**, *119*, 7605–7606.
- (11) Wylie, R. S.; Macartney, D. H. *J. Am. Chem. Soc.* **1992**, *114*, 3136–3138.
- (12) (a) Choi, H. S.; Huh, K. M.; Ooya, T.; Yui, N. *J. Am. Chem. Soc.* **2003**, *125*, 6350–6351. (b) Choi, H. S.; Ooya, T.; Sasaki, S.; Yui, N. *Macromolecules* **2003**, *36*, 5342–5347. (c) Fujita, H.; Ooya, T.; Yui, N. *Macromolecules* **1999**, *32*, 2534–2541.
- (13) (a) Yamaguchi, I.; Osakada, K.; Yamamoto, T. *Macromolecules* **1997**, *30*, 4288–4294. (b) Yamaguchi, I.; Takenaka, Y.; Osakada, K.; Yamamoto, T. *Macromolecules* **1999**, *32*, 2051–2054. (c) Yamaguchi, I.; Osakada, K.; Yamamoto, T. *Macromolecules* **2003**, *36*, 2742–2747.
- (14) (a) Shuai, X.; Porbeni, F. E.; Wei, M.; Bullions, T.; Tonelli, A. E. *Macromolecules* **2002**, *35*, 3126–3132. (b) Abdala, A. A.; Tonelli, A. E.; Khan, S. A. *Macromolecules* **2003**, *36*, 7833–7841. (c) Rusa, C. C.; Fox, J.; Tonelli, A. E. *Macromolecules* **2003**, *36*, 2742–2747.
- (15) (a) Jiao, H.; Goh, S. H.; Valiyaveetil, S. *Macromolecules* **2002**, *35*, 1399–1402. (b) Jiao, H.; Goh, S. H.; Valiyaveetil, S. *Macromolecules* **2002**, *35*, 3997–4002.
- (16) (a) Kakuchi, T.; Narumi, A.; Miura, Y.; Matsuya, S.; Sugimoto, N.; Satoh, T.; Kaga, H. *Macromolecules* **2003**, *36*, 3909–3913. (b) Kakuchi, T.; Narumi, A.; Matsuda, T.; Miura, Y.; Sugimoto, N.; Satoh, T.; Kaga, H. *Macromolecules* **2003**, *36*, 3914–3920.

wires tethered softly by metal ions are considered to have similarly high reactivities. This feature is due to the fact that their electronic structure will have occupied and unoccupied orbitals separated by infinitesimal differences in energy, which allow for mobile electrons but also increase the reactivity.^{23,24} Therefore, the use of a molecular insulating layer should permit these materials to attain the durability required for use in emerging molecular electronic technologies. However, the coordinative polyrotaxanes constructed directly by metal ions binding to the inclusion complexes formed between CDs and guest molecules have rarely been studied so far to the best of our knowledge. Our recent investigations indicated that the polymeric rotaxane like the missing link could be fabricated from the β -CD and 4,4'-dipyridine inclusion complex (**1**) with nickel(II) ions, which could be used as connectors for designing novel functional materials.²⁵ In the present paper, we further report a class of nanometer aggregations with the higher-order polypseudorotaxanes. These unique polypseudorotaxanes (**2**–**7**) are synthesized by the reaction of inclusion complex **1** with cobalt chloride, cobalt acetate, cobalt nitrate, zinc chloride, zinc acetate, and zinc nitrate, respectively, and their binding behaviors, nanostructures, and electrochemical properties are examined by ¹H NMR spectroscopy, circular dichroism, FT-IR, gel permeation chromatography, powder X-ray diffraction, thermogravimetric and differential thermal analysis, transmission electron microscopy, and cyclic voltammetry. The results obtained indicate that polypseudorotaxanes **2**–**7** could form different nanoarchitectures by the intermolecular self-assembly. Among them, polypseudorotaxanes **2**, **4**, and **7** show the nanosquare superstructures, and polypseudoro-

taxanes **3**, **5**, and **6** give the nanorod superstructures. These interesting results imply that the counteranions play critical roles in the formation of the polypseudorotaxane nanoarchitectures. Furthermore, the blue polypseudorotaxane **2** shows good electrochemical properties as a class of nanometer-scale soft material. The present investigations will serve to further our understanding of this developing, but less-investigated, area of electrochemical nanometer-scale soft materials by using β -CDs as the insulating layer.

Experimental Section

Materials. β -CD of reagent grade (Shanghai Reagent Factory) was recrystallized twice from water and dried in vacuo at 95 °C for 24 h prior to use. 4,4'-Dipyridine (DPD) was purchased from Acros and used as received. Cobalt chloride (CoCl₂·6H₂O), cobalt acetate (Co(CH₃COO)₂·4H₂O), cobalt nitrate (Co(NO₃)₂·6H₂O), zinc chloride (ZnCl₂), zinc acetate (Zn(CH₃COO)₂·2H₂O), and zinc nitrate (Zn(NO₃)₂·6H₂O) were commercially available and used without further purification.

Instruments. Elemental analyses were performed on a Perkin–Elmer 2400C instrument. ¹H NMR spectra were recorded in D₂O on a Varian Mercury VX300 spectrometer. FT-IR spectra were recorded on a Bio-Rad FTS 135 infrared spectrometer. The powder X-ray diffraction (XRD) patterns were obtained using a RIGAKU D/max-2500 diffractometer with Cu K α radiation ($\lambda = 1.5405 \text{ \AA}$). The thermogravimetric (TG) and differential thermal analysis (DTA) were recorded with a RIGAKU standard type instrument.

Transmission electron microscopy (TEM) experiments were performed using a Philips Tecnai G² 20 S-TWIN microscope operating at 200 kV. TEM samples were prepared by depositing a drop of the suspension onto a carbon grid.

Gel permeation chromatography (GPC) analysis was carried out with an HPLC workstation and Waters 410 differential refractometer equipped with PL Gel permeation columns. Water was used as an eluent at a flow rate of 0.8 mL min⁻¹ at 40 °C. Polystyrene standards were used to obtain a calibration curve.

Circular dichroism (CD) was recorded in a conventional quartz cell (light path 10 mm) on a JASCO J-715S spectropolarimeter equipped with a PTC-348WI temperature controller to keep the temperature at 25 °C. The polypseudorotaxanes were dissolved in aqueous solution with the concentration range of 5.0–8.0 $\times 10^{-5}$ mol dm⁻³ for the CD measurements.

The cyclic voltammetry (CV) measurements were performed on a BAS Epsilon electrochemical analyzer in a deoxygenated DMF solution containing 0.10 M *n*-Bu₄NPF₆ as a supporting electrolyte at 25 °C. The glassy carbon working electrode was polished with BAS polishing alumina suspension and rinsed with acetone before use. The counter electrode was a platinum wire. The measured potentials were recorded with respect to a Ag/AgNO₃ (0.01 M AgNO₃) reference electrode. In the experiments, the concentrations of polypseudorotaxanes **2**–**7** in DMF solutions containing [N(C₄H₉)₄]PF₆ (0.10 M) are 0.15 g L⁻¹. The sweep rate is 100 mV s⁻¹.

Polypseudorotaxane 2. Complex **1** was prepared by the reaction of DPD with β -CD in aqueous solution.²⁵ An aqueous solution (10 mL) of cobalt chloride (0.1 mmol) was added dropwise to an aqueous solution (20 mL) of **1** (0.1 mmol). The resulting mixture was then stirred at 40 °C for 7 h. The solvent was evaporated under a reduced pressure, and the precipitate formed was filtered off to give a blue powder. The crude product was recrystallized and purified from water and dried in vacuo to give **2** in 29% yield. FT-IR (KBr, cm⁻¹): ν 3335.0, 3060.6, 2923.2, 1734.1, 1650.0, 1607.2, 1559.2, 1538.8, 1490.9, 1456.5, 1417.4, 1367.9, 1332.7,

- (17) (a) Liu, Y.; Zhao, Y.-L.; Zhang, H.-Y.; Li, X.-Y.; Liang, P.; Zhang, X.-Z.; Xu, J.-J. *Macromolecules* **2004**, *37*, 6362–6369. (b) Liu, Y.; You, C.-C.; Zhang, H.-Y.; Kang, S.-Z.; Zhu, C.-F.; Wang, C. *Nano Lett.* **2001**, *1*, 613. (c) Liu, Y.; Li, L.; Fan, Z.; Zhang, H.-Y.; Wu, X.; Liu, S.-X.; Guan, X.-D. *Nano Lett.* **2002**, *2*, 257–261. (d) Liu, Y.; Wang, H.; Chen, Y.; Ke, C.-F.; Liu, M. *J. Am. Chem. Soc.* **2005**, *127*, 657–666. (e) Yang, Y.-W.; Chen, Y.; Liu, Y. *Inorg. Chem.* **2006**, *45*, 3014–3022.
- (18) (a) Taylor, P. N.; O'Connell, M. J.; McNeill, L. A.; Hall, M. J.; Aplin, R. T.; Anderson, H. L. *Angew. Chem., Int. Ed.* **2000**, *39*, 3456–3460. (b) Cacialli, F.; Wilson, J. S.; Michels, J. J.; Daniel, C.; Silva, C.; Friend, R. H.; Severin, N.; Samori, P.; Rabe, J. P.; O'Connell, M. J.; Taylor, P. N.; Anderson, H. L. *Nat. Mater.* **2002**, *1*, 160–164. (c) Michels, J. J.; O'Connell, M. J.; Taylor, P. N.; Wilson, J. S.; Cacialli, F.; Anderson, H. L. *Chem.-Eur. J.* **2003**, *9*, 6167–6176. (d) Wilson, J. S.; Frampton, M. J.; Michels, J. J.; Sardone, L.; Marletta, G.; Friend, R. H.; Samori, P.; Anderson, H. L.; Cacialli, F. *Adv. Mater.* **2005**, *17*, 2659–2663.
- (19) Shukla, A. D.; Bajaj, H. C.; Das, A. *Angew. Chem., Int. Ed.* **2001**, *40*, 446–448.
- (20) (a) Onagi, H.; Carrozzini, B.; Cascarano, G. L.; Easton, C. J.; Edwards, A. J.; Lincoln, S. F.; Rae, A. D. *Chem.-Eur. J.* **2003**, *9*, 5971–5977. (b) Onagi, H.; Blake, C. J.; Easton, C. J.; Lincoln, S. F. *Chem.-Eur. J.* **2003**, *9*, 5978–5988.
- (21) (a) Huskens, J.; Deij, M. A.; Reinhoudt, D. N. *Angew. Chem., Int. Ed.* **2002**, *41*, 4467–4471. (b) de Jong, M. R.; Huskens, J.; Reinhoudt, D. N. *Chem.-Eur. J.* **2001**, *7*, 4164–4170. (c) Nijhuis, C. A.; Huskens, J.; Reinhoudt, D. N. *J. Am. Chem. Soc.* **2004**, *126*, 12266–12267. (d) Crespo-Biel, O.; Dordi, B.; Reinhoudt, D. N.; Huskens, J. *J. Am. Chem. Soc.* **2005**, *127*, 7594–7600.
- (22) (a) van den Boogaard, M.; Bonnet, G.; van't Hof, P.; Wang, Y.; Brochon, C.; van Hutten, P.; Lapp, A.; Hadziioannou, G. *Chem. Mater.* **2004**, *16*, 4383–4385. (b) Han, B.-H.; Antonietti, M. *Chem. Mater.* **2002**, *14*, 3477–3485. (c) Lambert, J. B.; Liu, C.; Boyne, M. T.; Zhang, A. P.; Yin, Y. *Chem. Mater.* **2003**, *15*, 131–145.
- (23) Wudl, F. *Acc. Chem. Res.* **1984**, *17*, 227–232.
- (24) Frommer, J. E. *Acc. Chem. Res.* **1986**, *19*, 2–9.
- (25) Liu, Y.; Zhao, Y.-L.; Zhang, H.-Y.; Song, H.-B. *Angew. Chem., Int. Ed.* **2003**, *42*, 3260–3263.

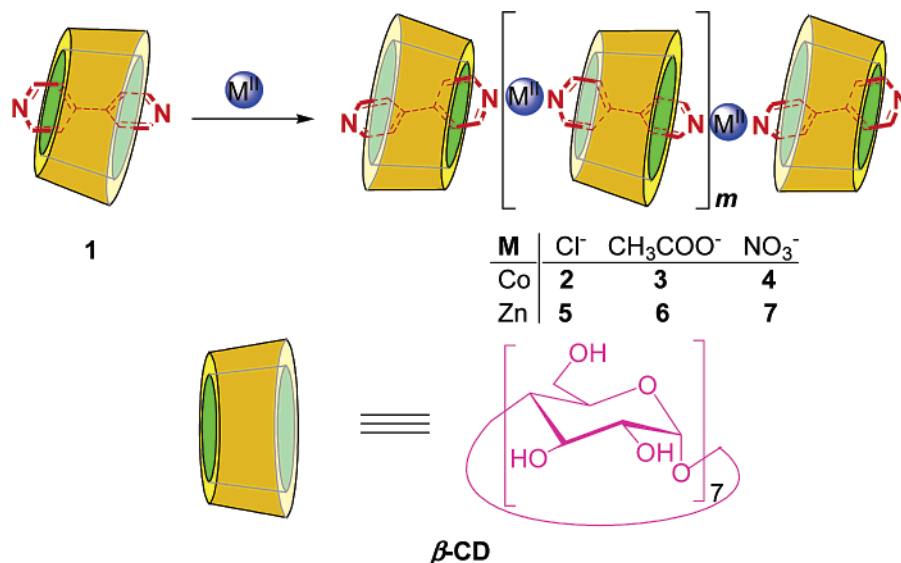


Figure 1. Schematic representation of the formation of polypseudorotaxanes 2–7.

1300.7, 1250.5, 1220.9, 1156.2, 1078.8, 1029.1, 941.9, 846.9, 809.0, 758.0, 707.6, 633.5, 610.5, 577.7, 530.2. Powder X-ray diffraction (XRD): 5.9° 2θ (d 14.87 Å), 6.3 (14.06), 9.0 (9.86), 9.7 (9.09), 10.6 (8.31), 11.7 (7.57), 12.5 (7.10), 14.7 (6.03), 15.4 (5.73), 16.0 (5.52), 17.1 (5.18), 17.7 (5.00), 18.8 (4.71), 19.5 (4.54), 20.9 (4.25), 21.5 (4.14), 22.8 (3.89), 24.5 (3.63), 25.7 (3.46), 27.1 (3.29), 28.8 (3.10), 31.3 (2.86), 34.3 (2.62), 40.2 (2.24). ¹H NMR (300 MHz, D₂O, TMS): δ 3.39–3.80 (m, 42H), 4.90–4.91 (d, 7H), 7.62 (s, 4H), 8.50 (s, 4H). Anal. Calcd for (C₅₂H₇₈O₃₅N₂CoCl₂·11H₂O)_{*n*}: C, 38.57; H, 6.22; N, 1.73. Found: C, 38.58; H, 6.50; N, 2.09.

Polypseudorotaxane 3. Pink **3** was prepared from **1** and cobalt acetate (Co(CH₃COO)₂·4H₂O), according to procedures similar to those described above, in 33% yield. FT-IR (KBr, cm⁻¹): ν 3323.3, 3068.3, 2927.0, 1594.0, 1567.5, 1551.6, 1534.6, 1443.5, 1426.6, 1332.7, 1300.7, 1241.1, 1155.5, 1079.5, 1030.5, 944.2, 852.7, 810.4, 756.4, 705.7, 611.2, 578.5, 530.8, 443.8. Powder X-ray diffraction (XRD): 6.4° 2θ (d 13.89 Å), 6.6 (13.30), 8.9 (9.91), 9.5 (9.30), 10.7 (8.28), 11.9 (7.46), 12.8 (6.93), 13.4 (6.59), 14.2 (6.25), 15.4 (5.73), 18.2 (4.88), 18.7 (4.74), 19.6 (4.53), 20.4 (4.36), 23.6 (3.76), 24.2 (3.67), 24.9 (3.57), 27.6 (3.23), 31.0 (2.88), 36.5 (2.46). ¹H NMR (300 MHz, D₂O, TMS): δ 1.82 (s, 6H), 3.34–3.75 (m, 42H), 4.85–4.86 (d, 7H), 7.57 (s, 4H), 8.46 (s, 4H). Anal. Calcd for (C₅₂H₇₈O₃₅N₂Co(CH₃COO)₂·7H₂O)_{*n*}: C, 42.19; H, 6.20; N, 1.76. Found: C, 42.36; H, 6.21; N, 2.08.

Polypseudorotaxane 4. Pink **4** was prepared from **1** and cobalt nitrate (Co(NO₃)₂·6H₂O), according to procedures similar to those described above, in 41% yield. FT-IR (KBr, cm⁻¹): ν 3336.8, 2927.9, 1608.6, 1415.7, 1361.7, 1334.7, 1153.4, 1080.1, 1029.9, 945.1, 852.5, 810.1, 756.1, 705.9, 609.5, 578.6, 528.5. Powder X-ray diffraction (XRD): 6.1° 2θ (d 14.57 Å), 7.2 (12.34), 10.1 (8.79), 11.9 (7.46), 12.2 (7.25), 14.5 (6.12), 15.6 (5.66), 17.7 (5.01), 18.8 (4.72), 20.0 (4.49), 21.4 (4.15), 23.8 (3.73), 25.1 (3.53), 26.1 (3.42), 29.1 (3.06), 34.5 (2.59), 37.0 (2.42), 38.0 (2.37). ¹H NMR (300 MHz, D₂O, TMS): δ 3.51–3.86 (m, 42H), 4.97–5.01 (d, 7H), 7.74 (s, 4H), 8.62 (s, 4H). Anal. Calcd for (C₅₂H₇₈O₃₅N₂Co(NO₃)₂·7H₂O)_{*n*}: C, 39.03; H, 5.79; N, 3.50. Found: C, 38.74; H, 6.02; N, 3.32.

Polypseudorotaxane 5. Colorless **5** was prepared from **1** and zinc chloride (ZnCl₂), according to procedures similar to those described above, in 37% yield. FT-IR (KBr, cm⁻¹): ν 3348.4, 2924.0, 1944.2, 1612.4, 1535.3, 1415.7, 1330.8, 1300.0, 1219.0, 1157.2, 1076.2, 1029.9, 945.1, 856.4, 810.1, 756.1, 705.9, 640.4, 609.5, 578.6, 528.5. Powder X-ray diffraction (XRD): 4.5° 2θ (d

19.80 Å), 6.2 (14.34), 9.0 (9.01), 9.7 (9.11), 10.7 (8.32), 11.9 (7.51), 12.4 (7.11), 14.1 (6.00), 14.7 (6.03), 15.3 (5.77), 16.1 (5.51), 17.1 (5.19), 17.6 (5.03), 18.8 (4.73), 19.5 (4.54), 20.7 (4.28), 21.4 (4.14), 23.0 (3.87), 23.5 (3.78), 24.1 (3.67), 24.9 (3.57), 27.1 (3.29), 28.4 (3.12), 31.0 (2.88), 32.0 (2.80), 34.7 (2.58), 36.8 (2.44), 40.8 (2.21), 43.5 (2.08), 44.4 (2.04). ¹H NMR (300 MHz, D₂O, TMS): δ 3.55–3.89 (m, 42H), 4.97–5.02 (d, 7H), 7.77 (s, 4H), 8.65–8.66 (d, 4H). Anal. Calcd for (C₅₂H₇₈O₃₅N₂ZnCl₂·8H₂O)_{*n*}: C, 39.74; H, 6.03; N, 1.78. Found: C, 39.46; H, 6.25; N, 2.03.

Polypseudorotaxane 6. Colorless **6** was prepared from **1** and zinc acetate (Zn(CH₃COO)₂·2H₂O), according to procedures similar to those described above, in 34% yield. FT-IR (KBr, cm⁻¹): ν 3332.9, 2927.9, 1593.1, 1419.6, 1369.4, 1334.7, 1300.0, 1242.1, 1153.4, 1080.1, 1033.8, 945.1, 848.7, 806.2, 756.1, 705.9, 613.4, 578.6, 528.5. Powder X-ray diffraction (XRD): 6.1° 2θ (d 14.62 Å), 7.2 (12.30), 10.1 (8.77), 11.8 (7.48), 12.2 (7.25), 14.3 (6.16), 15.6 (5.67), 17.6 (5.02), 18.8 (4.73), 20.1 (4.43), 21.4 (4.16), 24.0 (3.74), 26.0 (3.43), 26.7 (3.34), 29.4 (3.08), 34.4 (2.60), 37.7 (2.41). ¹H NMR (300 MHz, D₂O, TMS): δ 1.88 (s, 6H), 3.53–3.90 (m, 42H), 4.96–5.01 (d, 7H), 7.77 (s, 4H), 8.65 (s, 4H). Anal. Calcd for (C₅₂H₇₈O₃₅N₂Zn(CH₃COO)₂·9H₂O)_{*n*}: C, 41.09; H, 6.28; N, 1.71. Found: C, 40.97; H, 6.43; N, 1.59.

Polypseudorotaxane 7. Colorless **7** was prepared from **1** and zinc nitrate (Zn(NO₃)₂·6H₂O), according to procedures similar to those described above, in 39% yield. FT-IR (KBr, cm⁻¹): ν 3336.8, 2924.0, 1612.4, 1419.6, 1365.6, 1330.8, 1238.2, 1153.4, 1080.1, 1029.9, 945.1, 856.4, 810.1, 756.1, 705.9, 609.5, 578.6, 528.5, 482.2. Powder X-ray diffraction (XRD): 6.1° 2θ (d 14.62 Å), 7.2 (12.34), 10.0 (8.80), 11.8 (7.49), 12.2 (7.26), 14.5 (6.13), 15.6 (5.68), 17.6 (5.02), 18.7 (4.74), 19.9 (4.46), 21.3 (4.16), 23.9 (3.71), 26.0 (3.43), 34.5 (2.59), 37.1 (2.42), 37.9 (2.37). ¹H NMR (300 MHz, D₂O, TMS): δ 3.55–3.89 (m, 42H), 4.98–5.02 (d, 7H), 7.78 (s, 4H), 8.65–8.66 (d, 4H). Anal. Calcd for (C₅₂H₇₈O₃₅N₂Zn(NO₃)₂·12H₂O)_{*n*}: C, 36.81; H, 6.06; N, 3.30. Found: C, 36.59; H, 6.27; N, 2.98.

Results and Discussion

Synthesis. Polypseudorotaxanes 2–7 are prepared by the coordination of complex **1** and cobalt(II) or zinc(II) ions with different anions in 29–41% yields in aqueous solution, according to the procedures shown in Figure 1. The obtained polypseudorotaxanes could be easily separated by filtration

Table 1. GPC Detail Results for the Average Molecular Weight and Polymerization Degrees (n) of Polypseudorotaxanes 2–7

	M_n	M_w	$M_z + 1$	$(M_z + 1)/M_w$	polydispersity	n
2	13 025	14 934	20 089	1.35	1.15	9
3	7244	8124	9504	1.17	1.12	5
4	11 524	12 498	14 578	1.17	1.11	8
5	23 364	24 457	26 836	1.10	1.09	16
6	19 548	20 496	23 715	1.16	1.18	13
7	22 048	23 665	25 379	1.07	1.12	14

and purified by recrystallization. These polypseudorotaxanes are characterized by ^1H NMR spectroscopy, elemental analysis, FT-IR, gel permeation chromatography, powder X-ray diffraction, thermogravimetric and differential thermal analysis, and transmission electron microscopy, which are described as follows.

To confirm the coordination between inclusion complex **1** and metal ions, we performed ^1H NMR experiments at 25 °C in D_2O to give chemical shifts for **2–7** ($5.4\text{--}7.1 \times 10^{-4}$ mol dm^{-3}). Relative to complex **1**, meta protons of DPD are deshielded by about 0.03–0.18 ppm and ortho protons are shielded by about 0.03–0.16 ppm in the presence of the metal ions, suggesting that nitrogen atoms must coordinate with the metal ions.^{11,26} On the other hand, as compared with **1**, the IR spectra of **2–7** show that the C=N stretching vibration in DPD is shifted from 1595.3 to 1607.2, 1594.0, 1608.6, 1612.4, 1593.1, and 1612.4 cm^{-1} , respectively, which could also be ascribed to the coordination of the metal ions (M^{2+}). The 1:1 **1**: M^{2+} coordination in **2–7** is validated by the results of elemental analyses and UV–vis titration experiments. The spectrophotometric titrations are performed to determine the complex stoichiometry for the coordination of complex **1** with Co^{2+} or Zn^{2+} ions. The job plots for the **1**/ Co^{2+} (or **1**/ Zn^{2+}) system display a maximum at 0.5, which corresponds to 1:1 **1**/ Co^{2+} (or **1**/ Zn^{2+}) stoichiometry.

Furthermore, the average molecular masses of polypseudorotaxanes **2–7** are determined by gel permeation chromatography (GPC) analysis using water as an eluent, and the obtained results are shown in Table 1. According to the results of GPC experiments and elemental analysis, we could evaluate the polymerization degrees (n) of polypseudorotaxanes by using eq 1

$$n = M_w/M_c \quad (1)$$

$$M_c = M_1 + M_m + M_h \quad (2)$$

where M_w indicates the average molecular weight of polypseudorotaxanes obtained from the GPC experiments; M_c indicates the weight of a molecular complex unit including the weight (M_1) of molecular complex **1**, the weight (M_m) of a molecular metal salt with counterion, and the weight (M_h) of included water molecules. The obtained results show that the polymerization degrees of the polypseudorotaxanes are 9 for **2**, 5 for **3**, 8 for **4**, 16 for **5**, 13 for **6**, and 14 for **7**; these results are listed in Table 1.

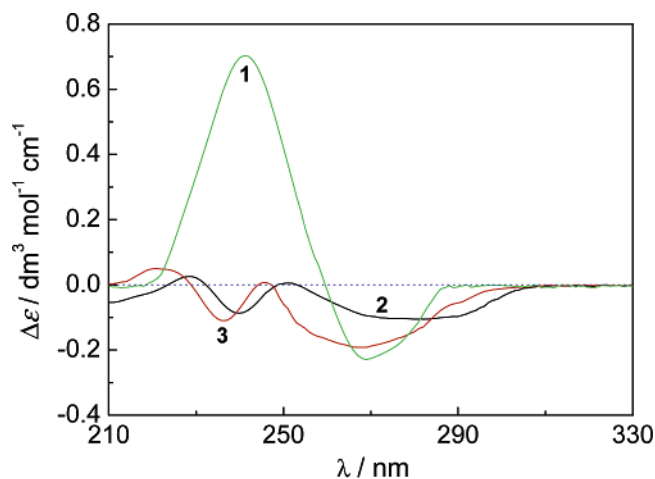


Figure 2. Circular dichroism spectra of complex **1** (7.9×10^{-4} mol dm^{-3}) and polypseudorotaxanes **2** (6.3×10^{-4} mol dm^{-3}) and **3** (5.8×10^{-4} mol dm^{-3}) in aqueous solution at 25 °C.

ICD Spectra. Interestingly, the coordination of metal ions with **1** results in different induced circular dichroism (ICD) spectra. Typically (Figure 2), the circular dichroism spectrum of **1** shows a strong positive Cotton effect peak at 241 nm ($\Delta\epsilon = 0.70$ dm^{-3} mol^{-1} cm^{-1}) and a negative Cotton effect at 269 nm ($\Delta\epsilon = -0.23$ dm^{-3} mol^{-1} cm^{-1}). However, the DPD molecules in β -CD cavities tethered by Co^{2+} ions give the opposite ICD signal: two negative Cotton effects at 240 nm ($\Delta\epsilon = -0.09$ dm^{-3} mol^{-1} cm^{-1}) and at 282 nm ($\Delta\epsilon = -0.11$ dm^{-3} mol^{-1} cm^{-1}) for **2**, and two negative Cotton effects at 242 nm ($\Delta\epsilon = -0.30$ dm^{-3} mol^{-1} cm^{-1}) and at 283 nm ($\Delta\epsilon = -0.10$ dm^{-3} mol^{-1} cm^{-1}) for **3** are observed, respectively. According to the pioneering studies of Kajtár,²⁷ Kim,²⁸ and Nau²⁹ et al., we could deduce that not only do the DPD molecules still lie in the cavities of β -CD after the formation of polypseudorotaxanes but also that the DPD moieties in the polypseudorotaxanes may become more acclivitous in the cavities of β -CD, leading to a sort of conformational change.

XRD, TG, and DTA. The powder X-ray diffraction (XRD) pattern of a sample could probe a large number of crystallites that are statistically oriented. In the present work, the XRD patterns of β -CD, DPD, and **1–7** are obtained by using a Rigaku D/max-2500 diffractometer with $\text{Cu K}\alpha$ radiation. The diffractogram of β -CD shows a characteristic reflection at $2\theta = 12.4^\circ$ ($d = 7.13$ Å), and that of DPD shows a characteristic reflection at $2\theta = 12.5^\circ$ ($d = 7.06$ Å). However, these characteristic reflections are changed to $2\theta = 11.8^\circ$ ($d = 7.49$ Å) and 12.1° ($d = 7.30$ Å) in the diffractogram of complex **1**, indicating that the arrangement of β -CD in **1** is changed by the introduction of DPD. Interestingly, the characteristic reflections at $2\theta = 11.7^\circ$ ($d = 7.57$ Å) and 12.5° ($d = 7.10$ Å) for **2**, $2\theta = 11.9^\circ$ ($d = 7.46$ Å) and 12.8° ($d = 6.93$ Å) for **3**, $2\theta = 11.9^\circ$ ($d = 7.46$ Å) and 12.2° ($d = 7.25$ Å) for **4**, $2\theta = 11.9^\circ$ ($d = 7.51$ Å)

(26) (a) Rekharsky, M.; Yamamura, H.; Kawai, M.; Inoue, Y. *J. Am. Chem. Soc.* **2001**, *123*, 5360–5361. (b) Yamamura, H.; Rekharsky, M. V.; Ishihara, Y.; Kawai, M.; Inoue, Y. *J. Am. Chem. Soc.* **2004**, *126*, 14224–14233. (c) Liu, Y.; Chen, Y.; Li, L.; Zhang, H.-Y.; Liu, S.-X.; Guan, X.-D. *J. Org. Chem.* **2001**, *66*, 8518–8527.

(27) Kajtár, M.; Horvath-Toro, C.; Kuthi, E.; Szejtli, J. *Acta Chim. Acad. Sci. Hung.* **1982**, *110*, 327–355.

(28) Park, K.-M.; Whang, D.; Lee, E.; Heo, J.; Kim, K. *Chem.—Eur. J.* **2002**, *8*, 498–508.

(29) (a) Zhang, X.; Nau, W. M. *Angew. Chem., Int. Ed.* **2000**, *39*, 544–547. (b) Mayer, B.; Zhang, X.; Nau, W. M.; Marconi, G. *J. Am. Chem. Soc.* **2001**, *123*, 5240–5248.

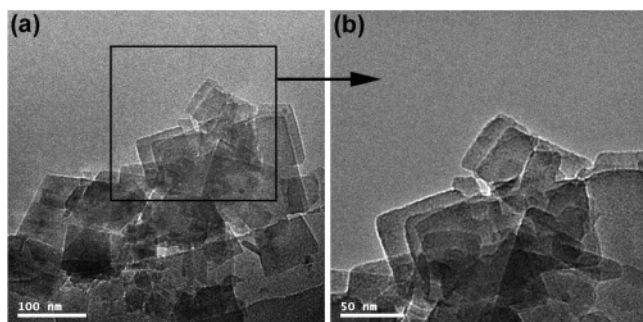


Figure 3. TEM images of polypseudorotaxane aggregation **2**, showing the square nanostructures.

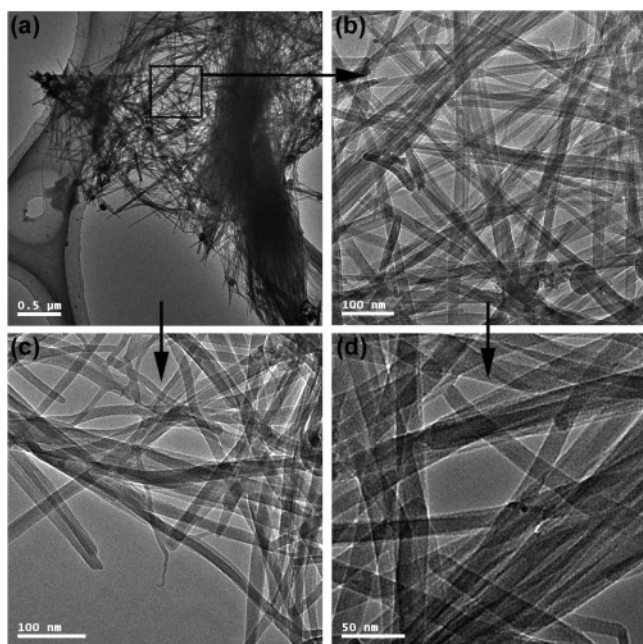


Figure 4. TEM images of polypseudorotaxane aggregation **3**, showing the rod nanostructures.

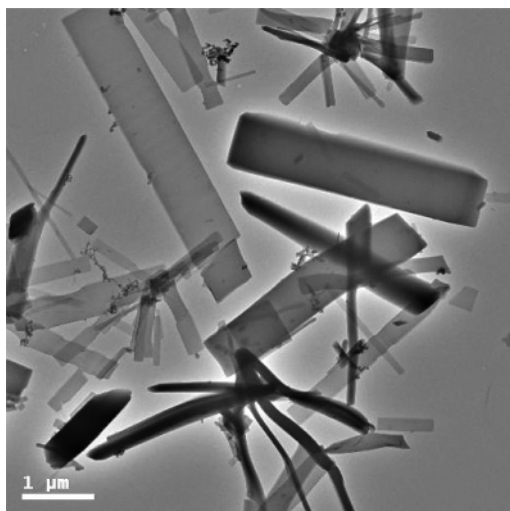


Figure 5. TEM images of polypseudorotaxane aggregation **4**, showing the square nanostructures.

and 12.4° ($d = 7.11 \text{ \AA}$) for **5**, $2\theta = 11.8^\circ$ ($d = 7.48 \text{ \AA}$) and 12.2° ($d = 7.25 \text{ \AA}$) for **6**, and $2\theta = 11.8^\circ$ ($d = 7.49 \text{ \AA}$) and 12.2° ($d = 7.26 \text{ \AA}$) for **7** appear in the diffractograms of polypseudorotaxanes, which shows that the coordination of metal ions make the β -CD and DPD reorient upon the

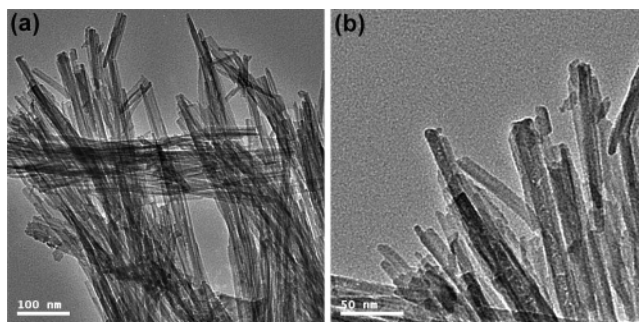


Figure 6. TEM images of polypseudorotaxane aggregation **5**, showing the rod nanostructures.

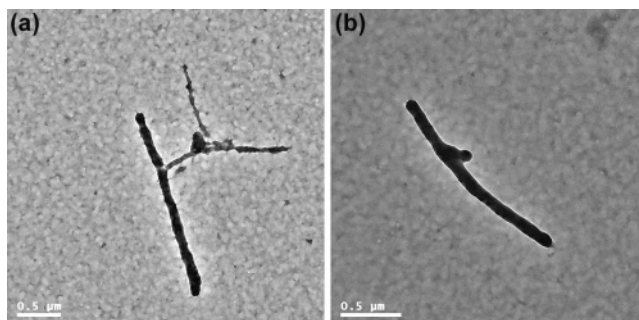


Figure 7. TEM images of polypseudorotaxane aggregation **6**, showing the rod nanostructures.

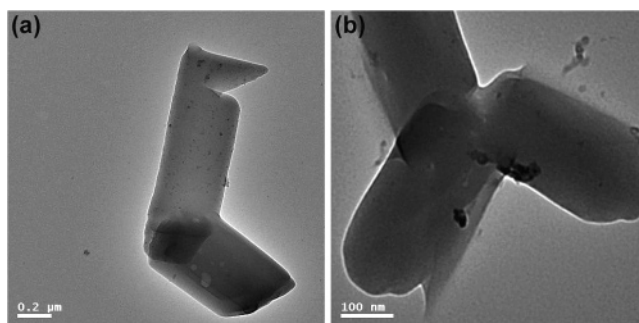


Figure 8. TEM images of polypseudorotaxane aggregation **7**, showing the square nanostructures.

formation of polypseudorotaxanes. Saenger³⁰ and Harata³¹ et al. reported that the crystal structures of CD complexes are classified mainly into three types: channel, cage, and layer. The β -CD-DPD complex was found to adopt a head-to-head channel type structure.^{25,32} The XRD characteristic reflection peaks of polypseudorotaxanes **2–7** are similar to those of β -CD-DPD complex **1** and different from those of β -CD. These results suggest that polypseudorotaxanes **2–7** might form head-to-head channel superstructures, which correspond to linear coordination modes.³³ The molecular modeling of polypseudorotaxanes with a short oligomer using

- (30) (a) McMullan, R. K.; Saenger, W.; Fayos, J.; Mootz, D. *Carbohydr. Res.* **1973**, *31*, 37–46. (b) Saenger, W. In *Inclusion Compounds*; Atwood, J. L., Davies, J. E. D., MacNicol, D. D., Eds.; Academic Press: London, 1984; Vol. 2, pp 231–259.
- (31) (a) Harata, K. *Chem. Rev.* **1998**, *98*, 1803–1827. (b) Harata, K. In *Comprehensive Supramolecular Chemistry*; Atwood, J. L., Davies, J. E. D., MacNicol, D. D., Vögtle, F., Eds.; Pergamon: Oxford, U.K., 1996; Vol. 3, pp 279–304.
- (32) (a) Liu, Y.; Zhao, Y.-L.; Zhang, H.-Y.; Yang, E.-C.; Guan, X.-D. *J. Org. Chem.* **2004**, *69*, 3383–3390. (b) Liu, Y.; Zhong, R.-Q.; Zhang, H.-Y.; Song, H.-B. *Chem. Commun.* **2005**, 2211–2213.
- (33) Okumura, H.; Kawaguchi, Y.; Harada, A. *Macromolecules* **2001**, *34*, 6338–6343.

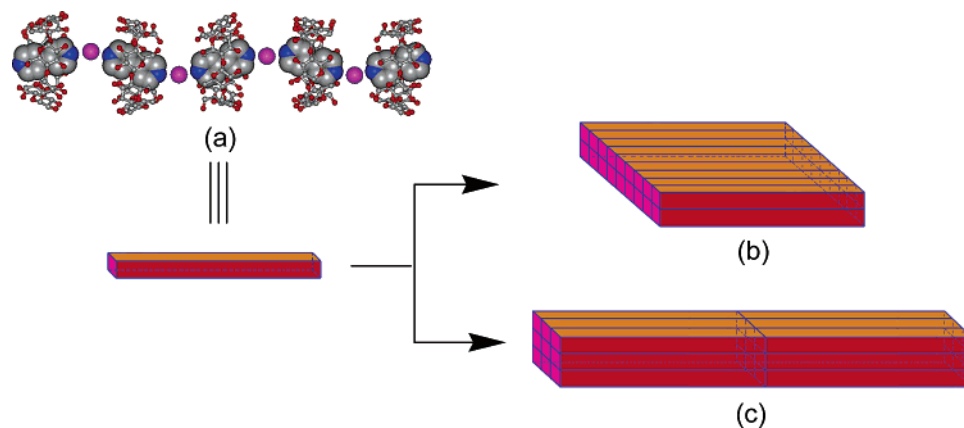


Figure 9. (a) Molecular modeling structure of a short oligomer of the polypseudorotaxanes, which are omitted anions. The DPD molecules are colored by atom type, with blue nitrogen atoms and gray carbon atoms. The β -CDs are also colored by atom type, with gray carbon atoms and red oxygen atoms. Metal ions are with pink. (b) Possible assembly mode for nanosquare superstructure of polypseudorotaxanes. (c) Possible assembly mode for nanorod superstructure of polypseudorotaxanes.

WebLab ViewerPro for Windows Molecular Modeling System is shown in Figure 9a.

To compare the thermal stabilities of **1–7**, we recorded the thermogravimetric (TG) and differential thermal analysis (DTA) with a RIGAKU standard type instrument. The decomposing temperatures of **1–7** are approximately 244, 210, 259, 238, 268, 246, and 252 °C, respectively, which may be ascribed to the dissociation of β -CD and DPD. Simultaneously, DTA results give an endothermic peak at ~ 333 °C (loses 87% of the original weight at 500 °C) for **1**, an exothermic peak at ~ 308 °C (loses 92.6% of the original weight at 600 °C) for **2**, an exothermic peak at ~ 303 °C (loses 91.3% of the original weight at 600 °C) for **3**, an exothermic peak at ~ 289 °C (loses 88.3% of the original weight at 600 °C) for **4**, an endothermic peak at ~ 307 °C (loses 97.7% of the original weight at 600 °C) for **5**, an endothermic peak at ~ 324 °C (loses 69.4% of the original weight at 600 °C) for **6**, and an endothermic peak at ~ 328 °C (loses 77.8% of the original weight at 600 °C) for **7**, which represent the temperatures of the decomposition of β -CD. The thermal dissociation temperatures indicate that the coordination effect of Co^{2+} or Zn^{2+} ions does not enhance the thermal stabilities of polypseudorotaxanes **2–7**.

TEM. Direct information about the shape and size of the polypseudorotaxane aggregates **2–7** in the solid state come from the transmission electron microscopy (TEM) results. The TEM images of polypseudorotaxane **2** are shown in Figure 3, from which it can be seen that the square nanostructures with the side length of 50–140 nm are distributed homogeneously. Similarly, polypseudorotaxanes **4** and **7** also show large-sized square (or rectangle) nanostructures, as can be seen from Figures 5 and 8. In sharp contrast, polypseudorotaxanes **3**, **5**, and **6** give nanorod superstructures (Figures 4, 6, and 7). Among them, the diameter of polypseudorotaxanes **3** and **5** are, respectively, 15–25 and 6–11 nm with uniform linear distribution, and **6** is 60–140 nm in diameter and 800–2000 nm in length.

It has been demonstrated that the polypseudorotaxane of β -CD-DPD with nickel chloride could form the nanorod superstructure.²⁵ In the present work, polypseudorotaxanes **2–7** show the nanorod or nanosquare morphologies. Therefore, it is interesting that these polypseudorotaxanes could

give two different nanoarchitectures. The results of TEM experiments suggest that the different sizes and shapes for the polypseudorotaxane aggregations may be attributed to the difference of both the metal ions and their counteranions, but on the basis of the results of XRD experiments, the coordination or dissociation of counteranions could not directly affect the linear coordination mode of polypseudorotaxanes. Upon the formation of inclusion complexes between CD and DPD, the conformation and coordination mode of DPD with metal ions are strictly limited, because of the bulky CD motif. Therefore, the smaller chloride and nitrate anions could take part in the coordination with metal ions in the formations of polypseudorotaxanes, whereas water molecules will coordinate instead of the larger acetate anion,³⁴ which may be the critical factor that results in the two different nanoarchitectural morphologies. That is to say, the noncoordinated acetate anion makes nanorod, and the coordinated chloride and nitrate anions make nanosquare except for polypseudorotaxane **5**. Figure 9 illustrates the possible assembly modes for the nanosquare/nanorod superstructures of polypseudorotaxanes. This concept will efficiently facilitate the design and synthesis of new supramolecular architectures with different morphologies by changing metal salts.

Colors and Electrochemical Properties. The color-change indicators are currently being sought for practical applications in the areas of analysis and materials science.^{35,36} Recently, Baglioni and co-worker reported the effect of cations and anions on the formation of polypseudorotax-

- (34) (a) Narnett, S. A.; Champness, N. R. *Coord. Chem. Rev.* **2003**, *246*, 145–168. (b) Barszcz, B. *Coord. Chem. Rev.* **2005**, *249*, 2259–2276. (c) Bradshaw, D.; Claridge, J. B.; Cussen, E. J.; Prior, T. J.; Rosseinsky, M. J. *Acc. Chem. Res.* **2005**, *38*, 273–282. (d) Leininger, S.; Olenyuk, B.; Stang, P. J. *Chem. Rev.* **2000**, *100*, 853–908. (e) Swiegers, G. F.; Malefetse, T. J. *Chem. Rev.* **2000**, *100*, 3483–3537.
- (35) (a) Ueno, A.; Kuwabara, T.; Nakamura, A.; Toda, F. *Nature* **1992**, *356*, 136–137. (b) Kuwabara, T.; Takamura, M.; Matsushita, A.; Ikeda, H.; Nakamura, A.; Ueno, A.; Toda, F. *J. Org. Chem.* **1998**, *63*, 8729–8735. (c) Aoyagi, T.; Nakamura, A.; Ikeda, H.; Ikeda, T.; Mihara, H.; Ueno, A. *Anal. Chem.* **1997**, *69*, 659–663. (d) Kuwabara, T.; Nakajima, H.; Nanasawa, M.; Ueno, A. *Anal. Chem.* **1999**, *71*, 2844–2849.
- (36) Ait-Haddou, H.; Wiskur, S. L.; Lynch, V. M.; Anslyn, E. V. *J. Am. Chem. Soc.* **2001**, *123*, 11296–11297.

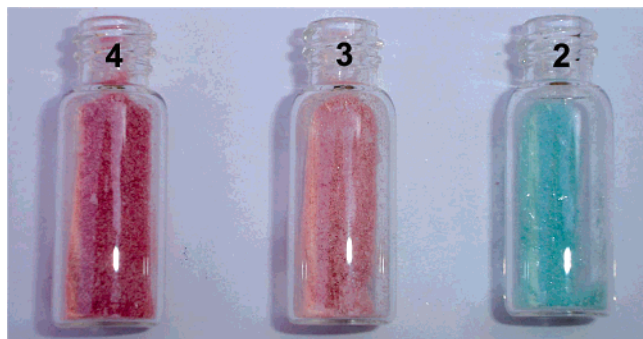


Figure 10. Colors of polypseudorotaxanes **2** (blue), **3** (pink), and **4** (pink).

anes.³⁷ In further studies, we find that polypseudorotaxanes **2–4** show different colors, i.e., blue for **2** and pink for **3** and **4**, as shown in Figure 10. Polypseudorotaxanes **5–7** are colorless. In control experiments, the 1:1 complexes of DPD with cobalt chloride, cobalt acetate, or cobalt nitrate all give pink. These observations suggest that there is no coordination between cobalt ions and water molecules in **2**; that is, besides the nitrogen atoms in DPD, only chloride anions participate in the coordination with Co^{2+} in **2**. One possible explanation is that, because the size of the chloride anion is smaller than that of the nitrate anion, the limited width between two cyclodextrins could allow for more than one chloride anion to coordinate with Co^{2+} , but does not allow for more than one nitrate anion to do so. Consequently, water molecules have to coordinate with Co^{2+} in the case of the nitrate anion.

Electrochemistry is a very powerful tool for monitoring supramolecular events such as supramolecular self-aggregation.³⁸ To investigate the electrochemical properties of polypseudorotaxanes **2–7**, we recorded the cyclic voltammograms (CVs) in a DMF solution of $[\text{N}(\text{C}_2\text{H}_5)_4]\text{BF}_6$. As can be seen from Figure 11, polypseudorotaxane **2** gives an electrochemical active cycle in the potential range between ca. -1.7 and ca. 1.0 V. The electrochemical curve shows a reduction wave at $E = 0.58$ V ($5.6 \mu\text{A}$, $6.7 \mu\text{C}$) and a reversible oxidation wave at $E = 0.77$ V ($29.6 \mu\text{A}$, $24.1 \mu\text{C}$). Moreover, the repeated scanning give almost the same curve (e.g., in the fifth scanning), indicating that polypseudorotaxane **2** is electrochemically stable. In contrast, polypseudorotaxanes **3** and **4** display almost electrochemical inactive cycles. Without CD units, the DPD-Co(II) complexes with different anions give fairly weak CV signals. On the basis of these phenomena, we deduce that the β -CD inclusion complexation and anion coordination with Co^{2+} could jointly effect the electrochemical properties of DPD- Co^{2+} complexes, resulting in satisfying electrochemical behavior of

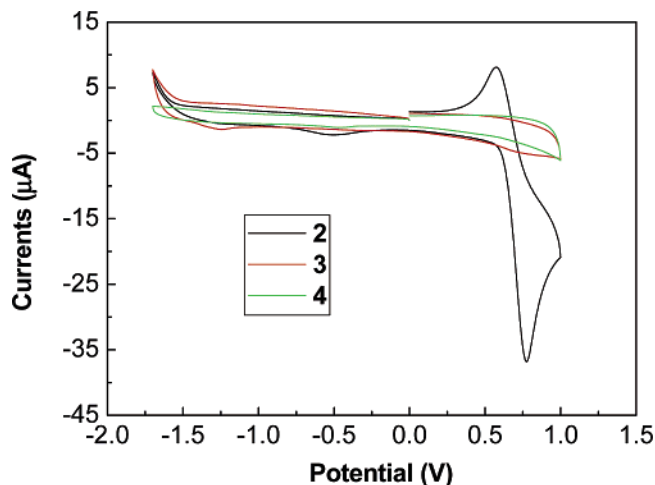


Figure 11. Cyclic voltammograms of polypseudorotaxanes **2–4** in DMF solution containing $[\text{N}(\text{C}_4\text{H}_9)_4]\text{PF}_6$. Sweep rate is 100 mV s^{-1} at 25°C .

polypseudorotaxane **2**. Furthermore, polypseudorotaxanes **5–7** with Zn^{2+} (see the Supporting Information) display almost-electrochemical inactive cycles.

Conclusion

In summary, we have prepared six polypseudorotaxanes **2–7** by using a simple method, i.e., Co^{2+} or Zn^{2+} ions binding with the resulting complexes of β -CDs and DPD molecules. The results obtained indicated that the polypseudorotaxanes do not only show two different nanoarchitectural morphologies, i.e., nanosquare or nanorod superstructures, but also possess the potential to be used as electrochemical materials, and thus represent a sample toward the construction of supramolecular aggregations with different coordination metal ions and counteranions. Although these studies have focused on the assembly and properties of the polypseudorotaxanes, the combination of these aggregations with emerging methods could expect to find many more intriguing applications.

Acknowledgment. This work was supported by NNSFC (90306009, 20421202, and 20372038) and the Tianjin Natural Science Foundation (043604411 and 05YFJMJC06500), which are gratefully acknowledged.

Note Added after ASAP Publication. There was an error in the sixth paragraph of the Experimental Section in the version published ASAP July 28, 2006; the corrected version was published ASAP August 3, 2006.

Supporting Information Available: The ^1H NMR spectra, FT-IR spectra, powder X-ray diffraction, and TG-DTA analysis of polypseudorotaxanes **2–7** and electrochemical curves of polypseudorotaxanes **5–7**. This material is available free of charge via the Internet at <http://pubs.acs.org>.

CM060933F

(37) Nostro, P. L.; Lopes, J. R.; Ninham, B. W.; Baglioni, P. *J. Phys. Chem. B* **2002**, *106*, 2166–2174.

(38) (a) Boulas, P. L.; Gómez-Kaifer, M.; Echegoyen, L. *Angew. Chem., Int. Ed.* **1998**, *37*, 216–247. (b) Cooke, G. *Angew. Chem., Int. Ed.* **2003**, *42*, 4860–4870.